Spectral dependence of photovoltaic currents in non-congruent LiNbO$_3$

Spectral dependence of photovoltaic currents in non-congruent LiNbO$_3$

A García-Cabañes and J M Cabrera

Departamento Física de Materiales C-IV, Universidad Autónoma de Madrid, Canto Blanco, Madrid E-28049, Spain

Abstract. The spectral response of the photovoltaic current has been studied in LiNbO$_3$ crystals of several stoichiometric compositions and reduction states. The height and shape of the spectra are found to depend substantially on stoichiometry. These dependences are parallel to those exhibited by the corresponding absorption spectra of the same crystals, and provide evidence that the photocurrent spectrum consists of several contributing bands. These results are compared with an analogous analysis of data on Fe-doped LiNbO$_3$. The photovoltaic transport length has been determined for specific component bands and found to be within the same order of magnitude for the measured stoichiometries and doping levels.

1. Introduction

The bulk photovoltaic effect in LiNbO$_3$ has been studied for many years, since it was first proposed by Glass and co-workers in 1974 [1] as an anisotropic scattering of electrons photoexcited from asymmetric electron traps. A major interest in the effect is connected with its relevance to the photorefractive recording process, since refractive index changes up to 10^{-3} can be obtained with photovoltaic transport only. The effect has been observed in LiNbO$_3$ doped with Fe^{3+} [1] and other 'photorefractive' impurities exhibiting charge transfer bands within the LiNbO$_3$ lattice [2]. It has also been observed in thermochemically reduced LiNbO$_3$, where it has been associated with bipolaron centres [3]. The association of the photovoltaic effect with specific impurities or centres is, then, generally accepted. Photovoltaic currents induced by x-ray excitation of 'pure' and iron-doped LiNbO$_3$ are not so well understood and are of lesser practical relevance [4,5].

However, the spectral response of the photovoltaic current is usually found to peak at energies higher than the absorption band peak of the corresponding donor centre. This striking effect has been theoretically interpreted in terms of the greater well asymmetry that the electron sees for higher photon energies, making the electron reach a higher momentum in the photocurrent direction for those photon energies [6]. It has also been found that the absorption bands associated with photovoltaic centres are complex [7]. They appear to heavily overlap with a broad absorption band (also complex) arising from thermochemical reduction, either intentionally produced or, most often, originating during the crystal growth process. These facts make it difficult to empirically separate contributions from independent bands as well as to check proposals made for the responsible centres.

In this paper, an experimental study of the spectral response of the photovoltaic current in nominally pure $LiNbO_3$ crystals of several stoichiometries and various reduction states will be presented for the first time. The use of crystals with different Li/Nb ratios has proved useful in overcoming the overlapping problem in the analysis of absorption spectra (by emphasizing some bands with respect to others) [7]. Thus, the component bands of the absorption spectra will be used to analyze the photocurrent spectra. Although this type of analysis is empirical, since unambiguous centre proposals are still missing, it is expected to provide a deeper understanding of the photovoltaic spectral response and to throw some light on the nature of those centres. The data will be compared with similar data on iron-doped samples.

2. Experimental methods

Non-congruent crystals, kindly provided by K Pólgar, were pulled at the Research Laboratory for Crystal Physics (Budapest, Hungary). Iron-doped crystals were pulled in our laboratory from a congruent melt (Li/Nb = 0.945) containing 0.1% mol of Fe_2O_3. High-purity chemicals from Johnson Matthey (Puratronic Grade I) were used as the starting material. Crystal blocks were x-ray oriented, poled, sawn and polished to obtain plates of size $1 \times 5 \times 10\,mm^3$, with their c axes parallel to the longer dimension of the large faces. Actual stoichiometry of non-congruent samples were determined by the absorption-edge method [8]. Table 1 gives details of the three samples used throughout this work. Unpolarized optical absorption spectra were taken with a Cary 2514 spectrophotometer from 300–2000 nm.

Table 1. Stoichiometry, doping and thermal treatments of used samples.

Sample	[Li]/[Nb]	Dopant (% mol)	Thermal treatment
1	0.998		Oxidation, 950 °C, 2 h
			Reduction, 880 °C, 2 h
2	0.972		Oxidation, 950 °C, 2 h
			Reduction, 900 °C, 2 h
3	0.945	0.1 Fe_2O_3	Oxidation, 900 °C, 2 h
			Reduction, 530 °C, 2 h
			Reduction, 750 °C, 2 h
			Reduction, 850 °C, 2 h

All samples were first oxidized by keeping them in an oxygen atmosphere, as indicated in table 1. After taking their optical absorption and photocurrent spectra, they were reduced in a vacuum (10^{-2} torr) at different temperatures, also as indicated in table 1. Heating and cooling rates ranged between 50–60 °C h^{-1} in all cases.

Short-circuit photocurrents of the samples along the c axis were measured with a Keithley Mod. 610C picoammeter with an ultimate sensitivity of 10^{-15} A. With the help of a stripchart recorder, the signal was left to reach a steady value (which it did after a few minutes) so that piroelectric and other non-photovoltaic contributions relaxed. Platinum-paste electrodes, painted onto the faces perpendicular to the c axis, were found to give reasonably good ohmic contacts. The sample and sample-holder were surrounded by a Faraday box (except for a small window for illumination) in

order to improve the signal-to-noise ratio of the small photocurrents. An internal resistance of $10^{10}\,\Omega$, much smaller than the resistance of the illuminated samples, was used in the electrometer. Samples were illuminated with unpolarized light with an intensity ranging between $5–20\,\mathrm{mW\,cm^{-2}}$ (depending on wavelength) and a bandwidth of about $20\,\mathrm{nm}$, by using an Applied Photophysics Irradiator model UV-90 (xenon lamp plus monochromator).

3. Results

3.1. Analysis of the data

To evaluate the photovoltaic current density from the experimental value given by the electrometer, two corrections have to be taken into account. First, the spectral dependence of the intensity of the illuminating system, which has been independently measured. Second, the geometrical shadow effect produced in the sample by self-absorption, combined with multiple reflections in the illuminated surfaces. A simple analysis gives the following expression for the photon flux per unit time inside the sample at the depth x starting from the front surface:

$$I(\lambda, x) = I_0(\lambda)\frac{1 - R(\lambda)}{1 - R^2(\lambda)e^{-2\alpha(\lambda)d}}\left[e^{-\alpha(\lambda)x} + R(\lambda)e^{-\alpha(\lambda)(2d-x)}\right]. \tag{1}$$

Here, $I_0(\lambda)$ is the photon flux per unit time coming from the illuminating system, which is assumed to be uniform on the front face, $R(\lambda)$ is the reflectivity, $\alpha(\lambda)$ is the absorption coefficient and d is the sample thickness along the illumination direction.

Assuming a single type of photovoltaic donor centre with concentration N_D, photon cross section σ, and photovoltaic transport length L_{pv}, the photovoltaic current density can be written as follows [9]:

$$j_{pv}(\lambda, x) = qL_{pv}\sigma(\lambda)N_D I(\lambda, x) = qL_{pv}\phi\alpha_{pv}(\lambda)I(\lambda, x) \tag{2}$$

where q is the electron charge, ϕ is the quantum efficiency of the photovoltaic process (L_{pv} and ϕ are assumed to be independent of wavelength), and $\alpha_{pv} = \sigma N_D/\phi$ is the absorption giving rise to a photovoltaic current. Notice that the coefficient $\alpha = \alpha_{pv} + \alpha_{npv}$ includes not only α_{pv}, but also other absorptions, α_{npv}, contributing to the geometrical shadow although producing no photocurrent. Integrating (2) over the thickness of the sample we finally obtain

$$j_{pv}(\lambda) = q\phi L_{pv}\alpha_{pv}(\lambda)I(\lambda) \tag{3}$$

with

$$I(\lambda) = I_0(\lambda)\frac{(1 - R)(1 - e^{-\alpha d})(1 + Re^{-\alpha d})}{\alpha d(1 - R^2 e^{-2\alpha d})} \tag{4}$$
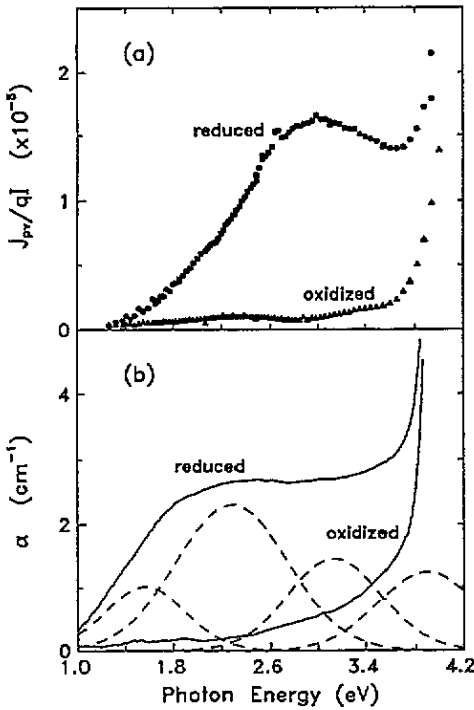
where α and R are wavelength dependent.

Figure 1. (*a*) Spectral response of the photocurrent density for a stoichiometric LiNbO$_3$ sample (Li/Nb = 1) reduced at 880 °C for 2 h. (*b*) Corresponding absorption spectra, including Gaussian components of the reduced spectrum.
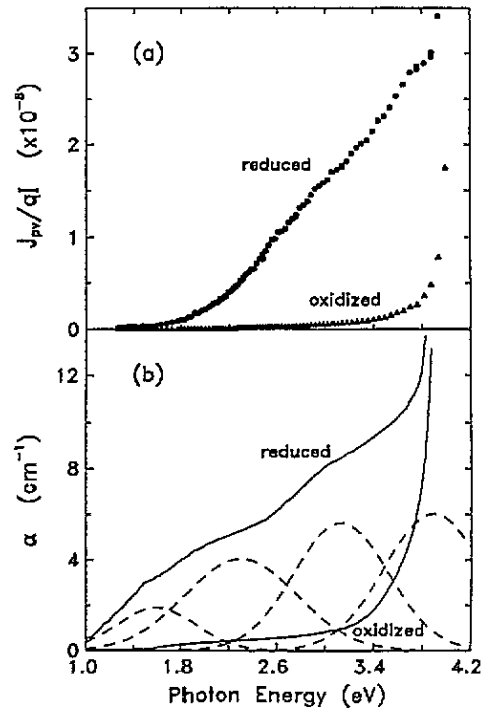
Figure 2. (*a*) Spectral response of the photocurrent density for a non-stoichiometric non-congruent LiNbO$_3$ sample (Li/Nb = 0.972) reduced at 900 °C for 2 h. (*b*) Corresponding absorption spectra, including Gaussian components of the reduced spectrum.

Table 2. Peaks and halfwidths of Gaussian components of absorption spectra.

Peak (eV)	Halfwidth (eV)	Samples
3.89	0.48	1, 2, 3
3.13	0.46	1, 2, 3
2.52	0.37	3
2.33	0.54	1, 2
1.59	0.39	1, 2

3.2. Spectral dependence of the photocurrent

Figures 1(*a*) and 2(*a*) show the spectral dependences of $j_{pv}/qI = \phi L_{pv}\alpha_{pv}$ in the oxidized and reduced states of the samples labelled 1 and 2 in table 1 (with Li/Nb ratios respectively of 1 and 0.972). For the purposes of comparison, in figures 1(*b*) and 2(*b*) the absorption spectra of the samples were included. Decompositions into Gaussian bands of the absorption changes induced by the reduction treatments were carried out according with data given in [7], and the results are also shown on these figures. For the sake of convenience, the peak positions and halfwidths of those component bands are included in table 2.

The photocurrent spectra in the oxidized state for both samples match the

respective absorption spectra to a high degree. This result indicates that a photovoltaic mechanism is operating for valence-band to conduction-band transitions. However, due to the strong self-absorption for $\alpha \gtrsim 40\,\text{cm}^{-1}$, the experimental values of the photocurrent only are reliable at the very beginning of the absorption edge. (Notice that for high α, the photovoltaic current is produced only within a very small fraction of the sample thickness d, and the use of (4) is not further reliable). In the reduced state, the photocurrent spectra appear shifted toward the high-energy side with respect to the corresponding absorption spectra. This behaviour is similar to that found by previous authors with spectra of iron- and copper-doped congruent LiNbO$_3$ [2, 10, 11]. Figures 3(a) and (b) show the photocurrent and absorption spectra of the iron-doped sample grown in our laboratory (sample 3 in table 1). The Gaussian decomposition according with [7] has also been included in figure 3(b). This helps in re-analyzing iron data reported by previous authors.
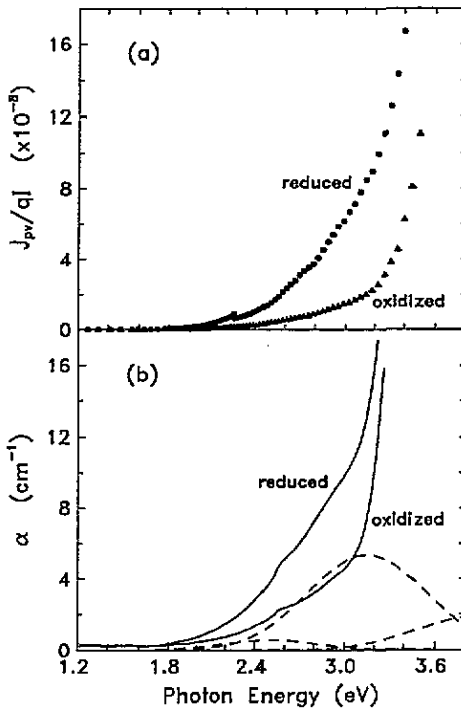

Figure 3. (a) Spectral response of the photocurrent density for an iron-doped LiNbO$_3$ sample reduced at 530 °C for 2 h. (b) Corresponding absorption spectra, including Gaussian components of the reduced spectrum.

In order to get a closer comparison between photocurrent and absorption spectra, decompositions of the photocurrent spectra were carried out using the same Gaussian bands previously used for the absorption spectra and listed in table 2. To avoid overlapping with the absorption-edge contribution, the oxidized-state spectra were subtracted from the reduced-state spectra. The fittings of the subtracted spectra are shown in figures 4(a), (b) and (c) for the samples of figures 1, 2 and 3 respectively. A good agreement is obtained between experimental points and fitted curves by varying

only the heights of the Gaussian bands. The heights obtained for each individual component of the photocurrent and absorption spectra can now be compared and, by using (3), the product ϕL_{pv} can be determined for each one. Table 3 lists the values of ϕL_{pv} for all the Gaussian components (except for the 3.9 eV band) in the three crystals studied. The value for the band peaked at 3.9 eV has not been included, since the heavy overlapping of this band with the absorption edge makes the analysis unreliable. The contribution to the photovoltaic current of the component peaked at 1.59 eV, which is present in all absorption spectra of pure crystals, has been found to be negligible. For comparison purposes a congruent sample, purchased from Crystal Technology and reduced to $\alpha(2.5\,\text{eV}) = 8.8\,\text{cm}^{-1}$, was also measured and gave the same values of ϕL_{pv}, within the experimental error, as those given in table 3. All these values also compare well with published data [12] on Fe- and Cu-doped samples where $\phi L_{pv} = 8 \times 10^{-9}\,\text{cm}$ and $2 \times 10^{-9}\,\text{cm}$ respectively.
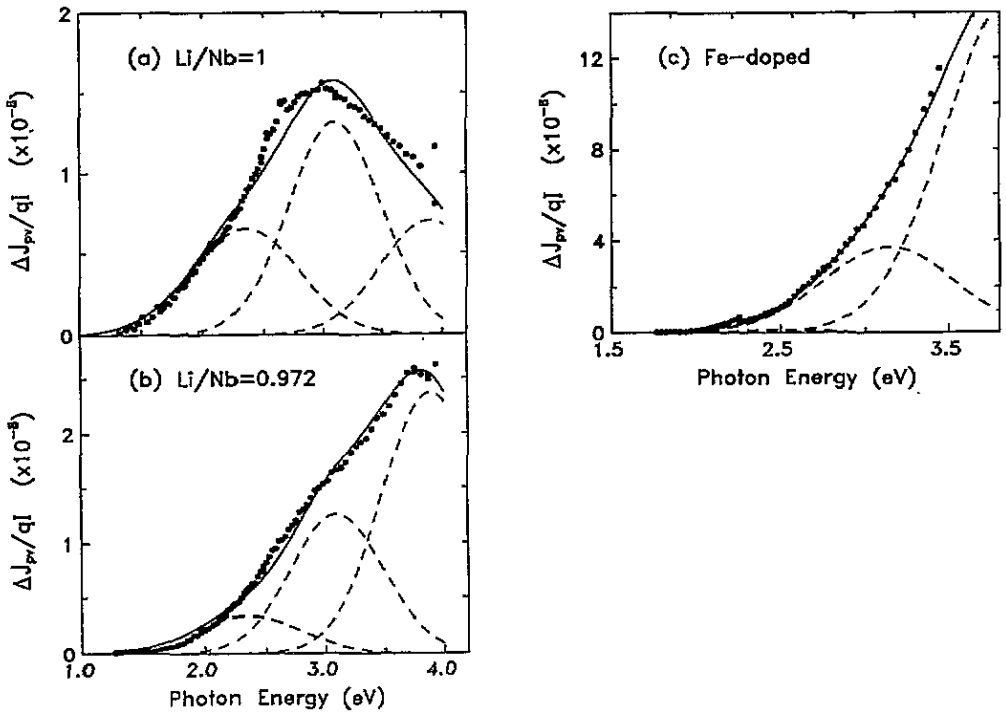

Figure 4. Gaussian components of photocurrent spectra of reduced samples after subtraction of those corresponding to oxidized spectra. (a), (b) and (c) correspond to figures $1(a)$, $2(a)$ and $3(a)$ respectively.

Table 3. Value of the product ϕL_{pv} ($10^{-9}\,\text{cm}$) for each Gaussian band.

Bands (eV)	Sample 1	Sample 2	Sample 3
3.13	9.1	2.2	9.9
2.52			1.7
2.33	2.8	0.8	

An accurate quantitative comparison between different samples is difficult because of the poor control of some experimental variables on changing from sample to sample. Examples of such variables are the electrode configuration, the spatial distribution of the illuminating light, and the absorption inhomogeneities in non-congruent or doped samples. A better comparison between individual component bands of the photocurrent and absorption spectra can be obtained by using the same sample and changing its reduction state to get various absorption levels. To this end, the iron-doped sample, which provides a higher photocurrent and absorption, has been successively reduced at 530, 750 and 850 °C, and its photocurrent and absorption spectra taken at each stage. Figures 5(*a*) and (*b*) show the photocurrent peak as a function of the absorption peak for the component bands peaking at 2.5 eV and 3.1 eV. A good linearity is observed in both cases.
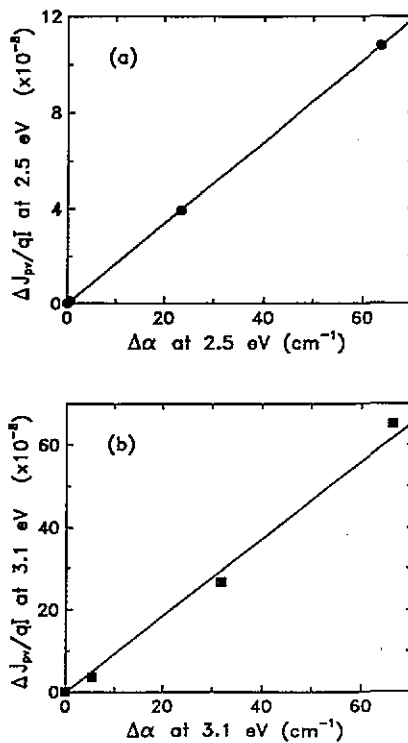

Figure 5. Photocurrent peak height as a function of the absorption peak height for the bands centred at 2.3 eV (*a*) and 3.1 eV (*b*) of the Fe-doped sample.

4. Discussion

The above data on LiNbO₃ samples with various stoichiometries and reduction states exhibit interesting features. As is the case with optical absorption spectra, previously reported [7], photocurrent spectra substantially depend on the stoichiometry and reduction level of the crystal, both in shape and height. In fact, a parallelism can be

established between corresponding absorption and photocurrent spectra, except for a shift toward the high-energy side of the latter. Theoretical calculations by Baltz and Kraut [6] suggest the shift is due to the additional energy the photon needs in order to transfer momentum to the excited electron in the required direction. As will be seen below, from the experimental results presented here a different and simpler interpretation can be proposed.

It has been shown above that several component bands actually contribute to the spectral response of the photovoltaic current. Moreover, those bands are the same as the Gaussian bands (both in peak positions and halfwidths) in which the corresponding absorption spectrum can be decomposed according to a previous paper [7]. Only the relative peak heights have to be changed to fit the photocurrent spectra, and this indicates different photovoltaic efficiencies of the different absorption components, as shown in table 3. Although such a decomposition is empirical and provides no *information about the nature of the microscopic centres giving rise to the photovoltaic current*, it strongly supports the occurrence of several centres contributing to the photocurrent.

This decomposition can also explain in a simple manner the 'shift' of the photocurrent peak toward higher energies (a greater efficiency of the components peaking on the high-energy side). Furthermore, by using only the Fe-doped sample at different reduction levels, a proportionality between the photocurrent and absorption peaks of corresponding individual bands has been found, as shown in figure 5. If the model proposed by Baltz and Kraut [6] were right, a similar proportionality should be found between the absorption peak at 2.5 eV and the photocurrent peak at 3.1 eV. However, this behaviour is not at all observed in experiment, as shown in figure 6. It has then to be concluded that there exists no 'shift' in the photocurrent spectra, but different photovoltaic efficiencies of the observed absorption components. This is also consistent with previous results showing the same spectral response for photorefractive recording and erasing in Fe-doped $LiNbO_3$ [13]. Since the photovoltaic current contributes to record but not to erase, a different spectrum should be observed if a 'shift' were present.
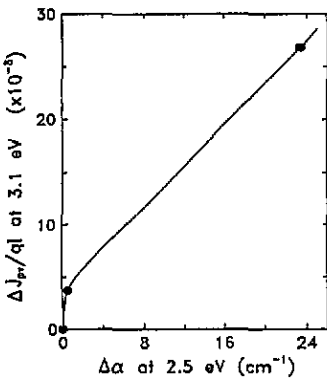

Figure 6. Peak height of the photocurrent band centred at 3.1 eV as a function of the peak height of the absorption band centred at 2.5 eV of the Fe-doped sample.

Another important finding is that the absorption band peaked at 1.59 eV does *not give rise to a photovoltaic current*. This band is commonly associated with small polarons Nb^{4+} [14] and is present in the absorption spectra of all pure crystals and
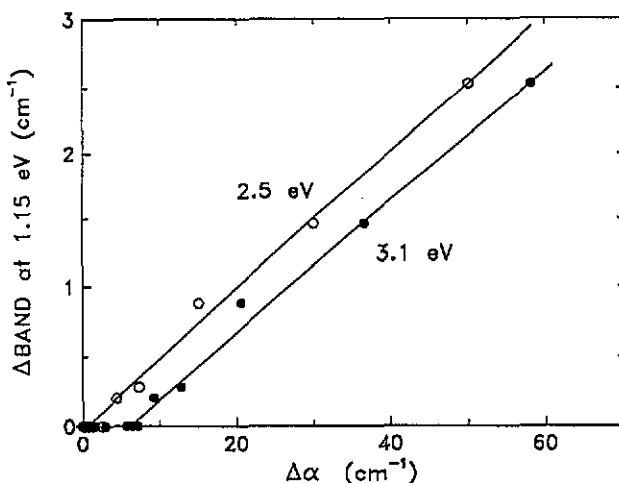
Figure 7. Absorption peaks of the 2.5 eV and 3.1 eV bands as a function of the infrared 1.15 eV band for the Fe-doped sample.

absent in those of Fe-doped crystals. Other authors [3] have attributed a photovoltaic current to this band, but the band they considered was the whole complex spectrum, so that independent effects of individual components were mixed.

The absolute values of ϕL_{pv}, as a measure of the photovoltaic efficiency of each individual component band (table 3), were obtained with poor accuracy because of a number of experimental uncertainties on changing from sample to sample. However, relative values for different bands obtained from the same sample are much more accurate and reliable. Thus, although the absolute value of ϕL_{pv} for the 3.1 eV component ranges from 2×10^{-9} cm to 9.9×10^{-9} cm (including congruent, non-congruent and doped samples), the ratio between the ϕL_{pv} values for the 3.1 eV and 2.3 eV components is 3.0 ± 0.2. It can then be concluded that the 3.1 eV band is the most efficient, no matter what the sample stoichiometry or doping, and its efficiency is about the same in all samples. This is a striking finding, since Fe-doped samples exhibit a photorefractive efficiency (with photovoltaic recording) several orders of magnitude higher than reduced pure congruent samples [15] where the 3.1 eV band is as intense as in Fe-doped samples. A plausible explanation is that Fe doping modifies the carrier mobility (via Fe^{3+} traps [16] or some other mechanism) to a smaller value. The opposite effect is produced by Mg doping, which increases the mobility, and so decreases the photorefractive efficiency with the same photovoltaic efficiency [16]. An increase of the carrier mobility upon reduction of congruent pure samples has also been reported [17], which would partly explain the smaller photorefractive efficiency of these samples. However, the reduction treatment was much stronger than those commonly used in photorefractive experiments, and further work is needed in this direction before a change of view as important as that proposed here can be confirmed.

Unfortunately, no answer can be obtained from our results to the important question of which are the specific centres giving rise to each component band and why their photovoltaic efficiencies are different. However, we make some comments based on the decomposition of the observed spectrum into several photovoltaic/absorption

bands. One can now be more precise and attribute the 2.5 eV component appearing in Fe-doped samples to the $Fe^{2+} \rightarrow Nb^{5+}$ charge-transfer transition. This band is present only in Fe-doped samples and, as shown in figure 7 for the set of reduction treatments, its intensity is proportional to the 1.15 eV infrared band, which has been proved to arise from an intra-ionic transition of the Fe^{2+} ion [18]. The 3.1 eV band, which appears in Fe-doped samples, also appears in all pure samples and, as shown in figure 7, is not proportional to the 1.15 eV band of Fe^{2+}. The 3.1 eV band should then be attributed to some intrinsic defect created during the reduction process, both in Fe-doped and pure crystals. The fact that this band is stronger in congruent crystals (with a higher concentration of anti-site Nb^{5+} ions) than in stoichiometric ones, suggests that it could be associated with anti-site Nb^{4+} with or without a nearest-neighbour oxygen vacancy.

Acknowledgments

References

[1] Glass A M, von Der Linde D and Negran T J 1974 *Appl. Phys. Lett.* **25** 233
[2] Krätzig E and Kurz H 1976 *Ferroelectrics* **13** 295
[3] Schirmer O F, Juppe S and Koppitz J 1987 *Cryst. Latt. Def. Amorph. Mat.* **16** 353
    Koppitz J, Schirmer O F and Kuznetsov A 1987 *Europhys. Lett.* **4** 1055
[4] Schirmer O F 1979 *J. Appl. Phys.* **50** 3404
[5] Chanussot G 1978 *Ferroelectrics* **20** 37
    Heyszenau H 1978 *Phys. Rev.* B **18** 1586
[6] von Baltz R and Kraut W 1981 *Phys. Rev.* B **23** 5590
[7] García-Cabañes A, Diéguez E, Cabrera J M and Agulló-López F 1989 *J. Phys.: Condens. Matter* **1** 6453
[8] Földvari I, Pólgar K, Voszka R and Balasanyan R N 1984 *Cryst. Res. Technol.* **19** 1659
[9] Carrascosa M and Agulló-López F 1986 *IEEE J. Quantum Electron.* **22** 1369
[10] Krätzig E and Kurz H 1976 *Ferroelectrics* **10** 159
[11] Krätzig E and Orlowsky R 1980 *Ferroelectrics* **27** 241
[12] Festl H G, Hertel P, Krätzig E and von Balzt R 1982 *Phys. Stat. Solidi* b **113** 157
[13] Baquedano J A, Carrascosa M, Arizmendi L and Cabrera J M 1987 *J. Opt. Soc. Am.* B **4** 309
[14] Arizmendi L, Cabrera J M and Agulló-López F 1984 *J. Phys. C: Solid State Phys.* **17** 515
[15] Phillips W, Amodei J J and Staebler D L 1972 *RCA Rev.* **33** 94
[16] Sommerfeldt R, Holtmann L, Krätzig E and Grabmaier B C 1988 *Phys. Stat. Solidi* a **106** 89
[17] Ohmori Y, Yasojima Y and Inuishi Y 1975 *Japan. J. Appl. Phys.* **14** 1291
[18] Bollmann W 1980 *Kristall Tech.* **15** K13